The V-ATPase V1 subunit A1 is required for rhodopsin anterograde trafficking in *Drosophila*

Haifang Zhao[a,b], Jing Wang[b], and Tao Wang[b,*]
[a]School of Life Sciences, Tsinghua University, Beijing 100084, China; [b]National Institute of Biological Sciences, Beijing 102206, China

ABSTRACT **Synthesis and maturation of the light sensor, rhodopsin, are critical for the maintenance of light sensitivity and for photoreceptor homeostasis. In *Drosophila*, the main rhodopsin, Rh1, is synthesized in the endoplasmic reticulum and transported to the rhabdomere through the secretory pathway. In an unbiased genetic screen for factors involved in rhodopsin homeostasis, we identified mutations in *vha68-1*, which encodes the vacuolar proton-translocating ATPase (V-ATPase) catalytic subunit A isoform 1 of the V1 component. Loss of *vha68-1* in photoreceptor cells disrupted post-Golgi anterograde trafficking of Rh1, reduced light sensitivity, increased secretory vesicle pH, and resulted in incomplete Rh1 deglycosylation. In addition, *vha68-1* was required for activity-independent photoreceptor cell survival. Importantly, *vha68-1* mutants exhibited phenotypes similar to those exhibited by mutations in the V0 component of V-ATPase, *vha100-1*. These data demonstrate that the V1 and V0 components of V-ATPase play key roles in post-Golgi trafficking of Rh1 and that *Drosophila* may represent an important animal model system for studying diseases associated with V-ATPase dysfunction.**

Monitoring Editor
Akihiko Nakano
RIKEN

Received: Sep 11, 2017
Revised: Apr 23, 2018
Accepted: Apr 30, 2018

INTRODUCTION

The vacuolar proton-translocating ATPase (V-ATPase) is composed of 14 different subunits that are organized into subcomplexes, namely, an ATP-catalyzing domain (V1) and a proton-translocation domain (V0). V-ATPase plays a major role in organelle acidification in eukaryotic cells (Forgac, 2007; Cotter *et al.*, 2015) and has been shown to regulate a number of other cellular processes, including membrane trafficking and protein degradation (Maxson and Grinstein, 2014; Cotter *et al.*, 2015). Recently, several studies have identified unusual and controversial functions of V-ATPase, implicating this protein in membrane fusion and neurotransmitter release (Peters *et al.*, 2001; Hiesinger *et al.*, 2005). It has been suggested that the physical presence of the V0 domain, and not the proton-translocation ability, is required for membrane fusion (Peters *et al.*, 2001; Bayer *et al.*, 2003; Baars *et al.*, 2007; Sreelatha *et al.*, 2015). However, several studies have claimed that acidification, rather than the physical presence of V0, is instead how the V0 domain contributes to vesicle fusion (Ungermann *et al.*, 1999; Coonrod *et al.*, 2013).

The major rhodopsin in *Drosophila*, Rh1, is synthesized in the endoplasmic reticulum (ER), where it undergoes N-linked glycosylation and strict quality control before being trafficked to the rhabdomeres, where it becomes a functionally active photon receptor (Satoh *et al.*, 1997; Wang and Montell, 2007). Proper targeting of Rh1 to the rhabdomere is crucial for normal phototransduction and photoreceptor cell survival (Colley *et al.*, 1995; Xiong and Bellen, 2013; Schopf and Huber, 2017). A wide array of chaperones within the ER ensure proper biosynthesis and folding of rhodopsin (Colley *et al.*, 1991; Rosenbaum *et al.*, 2006, 2011; Satoh *et al.*, 2015). After Rh1 exits the ER, it is subjected to additional quality control, including a series of deglycosylation events that are essential for the transport and function of newly synthesized rhodopsin (Cao *et al.*, 2011;

This article was published online ahead of print in MBoC in Press (http://www.molbiolcell.org/cgi/doi/10.1091/mbc.E17-09-0546) on May 9, 2018.

The authors declare no conflict of interest.

Author contributions: H.Z. and T.W. designed the experiments. H.Z. and J.W. performed the experiments. H.Z. and T.W. analyzed and interpreted the data. H.Z. and T.W. wrote the article.

*Address correspondence to: Tao Wang (wangtao1006@nibs.ac.cn).

Abbreviations used: dMppe, *Drosophila* metallophosphoesterase; DPP, deep pseudopupils; EMS, ethyl methanesulfonate; Endo H, endoglycosidase H; ER, endoplasmic reticulum; ERG, electroretinogram; IgG, immunoglobulin G; INAD, Inactivation no afterpotential D; MW, molecular weight; nSyb-mp, nSyb-mCherry-pHluorin reporter; PBS, phosphate-buffered saline; PFA, paraformaldehyde; PNGase F, peptide N-glycosidase F; RFP, red fluorescent protein; TRP, transient receptor potential; V-ATPase, vacuolar proton-translocating ATPase.

Rosenbaum *et al*., 2014). Rab11, which is present in the *trans*-Golgi network and post-Golgi vesicles, is required for trafficking from the Golgi to the apical rhabdomere membrane (Satoh *et al*., 2005; Xiong *et al*., 2012). However, other than the role played by Rab11, very little is known about how anterograde transport of rhodopsin from the Golgi to the rhabdomere is regulated.

Both active and intact V-ATPase is required for trafficking and processing of a variety of plasma membrane receptors, including components of the Wnt receptor complex, namely the G protein–coupled receptor Frizzled and LRP6 (Buechling *et al*., 2010; Cruciat *et al*., 2010; Hermle *et al*., 2010). A previous unbiased genetic screen for synaptic malfunction in *Drosophila* identified a mutation in *vha100-1* (*V0 Subunit a1*), which encodes the largest subunit of the V0 domain and regulates the formation of soluble *N*-ethylmaleimide–sensitive factor activating protein receptor (SNARE) complexes during vesicle exocytosis (Hiesinger *et al*., 2005; Wang *et al*., 2014a). Studies in *Drosophila*, *Caenorhabditis elegans*, and mammalian cells have directly implicated the V0 domain in secretory vesicle exocytosis, independent of the V1 domain (Hiesinger *et al*., 2005; Liegeois *et al*., 2006; Poea-Guyon *et al*., 2013). However, mutations in both V0 and V1 components have been reported to disrupt vesicular trafficking and deglycosylation of secretory proteins in cutis laxa patients, indicating a role for the V1 domain in vesicle exocytosis (Kornak *et al*., 2008; Hucthagowder *et al*., 2009; Van Damme *et al*., 2017).

In the present study, we performed ethyl methanesulfonate (EMS) mutagenesis in *Drosophila* and screened chromosome 2L for mutations that affect rhodopsin homeostasis and photoreceptor cell integrity using the "*Rh1::GFP ey-flp/hid*" method with in vivo fluorescence imaging of Rh1–green fluorescent protein (GFP) (Huang *et al*., 2015). A mutation in *vha68-1*, which encodes the V-ATPase catalytic subunit A (isoform 1) of the V1 subcomplex, was isolated. *vha68-1* mutants exhibited synaptic dysfunction, reduced light sensitivity, defective post-Golgi anterograde trafficking of rhodopsin, and light-independent retinal degeneration. Similar phenotypes are seen in *vha100-1* mutants. Our data reveal a conserved function of the V1 subcomplex in secretory vesicle exocytosis.

RESULTS

Vha68-1 is required for rhodopsin homeostasis and visual response

To identify genes involved in rhodopsin homeostasis, we performed EMS mutagenesis and screened chromosome 2L using the "*Rh1::GFP ey-flp/hid*" system (Supplemental Figure S1) (Huang *et al*., 2015). We generated homozygous mutant eyes in the heterozygous animal and examined fluorescence of GFP-tagged Rh1, the major rhodopsin in *Drosophila*. When wild-type eyes were examined using this system, they had intact deep pseudopupils (DPP), with six rhabdomeres clearly visible via optical neutralization, either 1 or 5 d following eclosion. We screened for mutants in which DPP fluorescence was largely reduced on day 1 and/or day 5 (Figure 1A).

In summary, among ~10,000 mutagenized flies, we identified ~50 alleles that affected Rh1 DPP fluorescence, including three new alleles of *ninaA* (*neither inactivation nor afterpotential A*), which clearly functions in rhodopsin biogenesis. For one complementation group that included two alleles, the DPP was completely lost, and the Rh1-GFP fluorescence signal was diffuse on both days 1 and 5 (Figure 1A). To identify the gene responsible for this phenotype, we performed chromosome 2L deficiency mapping, eventually localizing these mutations to the *vha68-1* genomic locus, which encodes one of the three *Drosophila* isoforms of the V-ATPase catalytic subunit A (isoform 1). We named these two alleles *vha68-1*^{1} and *vha68-1*^{2}. These two alleles both contain single-nucleotide changes within the coding region that alter a conserved amino acid of the Vha68 protein (Figure 1B and Supplemental Figure S2).

We next used immunohistochemistry to visualize the localization pattern of endogenous Rh1 in resin-embedded retinal sections. In wild-type flies, the majority of Rh1 localized exclusively to the rhabdomere, whereas in *vha68-1*^{1} photoreceptor cells, Rh1 accumulated in the cell body (Figure 1, C and D). This is also seen in *vha100-1*^{2} mutants. Moreover, expressing Vha68-1 in *vha68-1*^{1} photoreceptor cells via the *rh1* promoter (*ninaE: neither inactivation nor afterpotential E*) completely rescued Rh1 mislocalization. We then performed electroretinogram (ERG) recordings to analyze visual responses in *vha68-1*^{1} mutant animals. Exposing wild-type flies to orange light resulted in two discernible components in the ERG, namely, a photoreceptor-derived sustained corneal negative response and on and off transients reflecting synaptic transmission to second-order lamina neurons (Figure 1E). As has been reported for *vha100-1* mutants, which exhibit disrupted visual transmission (Hiesinger *et al*., 2005), both *vha68-1*^{1} and *vha100-1*^{2} mutants exhibited complete loss of on and off transients (Figure 1E). Expressing wild-type *vha68-1* via the *ubiquitin* (*ubi*) promoter in the *vha68-1*^{1} mutant fully restored on and off transients (Figure 1E). Moreover, *vha68-1*^{1} and *vha100-1*^{2} flies both displayed dramatic decreases in light sensitivity compared with wild-type flies, indicating that levels of functional rhodopsin were reduced in these two mutant flies (Figure 1F and Supplemental Figure S3A). Consistent with the light sensitivity data, Western blot analysis of *vha68-1*^{1} flies revealed reduced levels of total Rh1 (Supplemental Figure S3, B and C). Together with the accumulation of Rh1 in the cell body, these results demonstrate a large reduction in rhabdomeric rhodopsin in *vha68-1*^{1} mutant flies.

We next tested whether mutations in other V-ATPase subunits result in similar retinal phenotypes. As expected, because V-ATPase is essential for cellular homeostasis, many of these subunits were cell lethal when homozygous in the eye (Supplemental Table S1). According to our data, *vha68-1* and *vha100-1* were the only V-ATPase subunits for which this was not the case, as eye-specific loss of these genes resulted in retinas with defective ERG responses. This suggested that there are other genes with functions redundant to *vha68-1* and *vha100-1*. Similar to Vha100, which is encoded by five different genes, three conserved genes encode a V-ATPase catalytic subunit A, namely *vha68-1*, *vha68-2*, and *vha68-3* (Supplemental Figure S2). *vha68-1* is primarily expressed in the fly head, *vha68-2* is ubiquitously expressed, and *vha68-3* is expressed specifically in the testes, according to in situ hybridization analysis (Allan *et al*., 2005). To test whether *vha68-1* is functionally distinct from these other two genes, we used the *ninaE* promoter to drive expression of *vha68-2* and *vha68-3* in *vha68-1*^{1} photoreceptor cells. Both rescued Rh1 mislocalization (Figure 1C), suggesting that different Vha68 variants have the same function and that defects in Rh1 accumulation may result from loss of the major photoreceptor Vha68 protein.

Rh1 anterograde trafficking is slow in *vha68-1*^{1} photoreceptors

We next asked why Rh1 accumulated in cytoplasmic vesicles of *vha68-1*^{1} flies. Because V-ATPase sustains low pH within degradative cellular compartments, disruption of the key catalytic subunit of V1 may have disrupted the endolysosomal degradation of rhodopsin. Alternatively, because Vha100-1 is required for synaptic vesicle exocytosis, it is possible that mislocalization of Rh1 in *vha68-1*^{1} photoreceptors resulted from defective anterograde trafficking of membrane proteins (Hiesinger *et al*., 2005; Haberman *et al*., 2012). Rhodopsin, and the major downstream Ca^{2+}/cation channel TRP

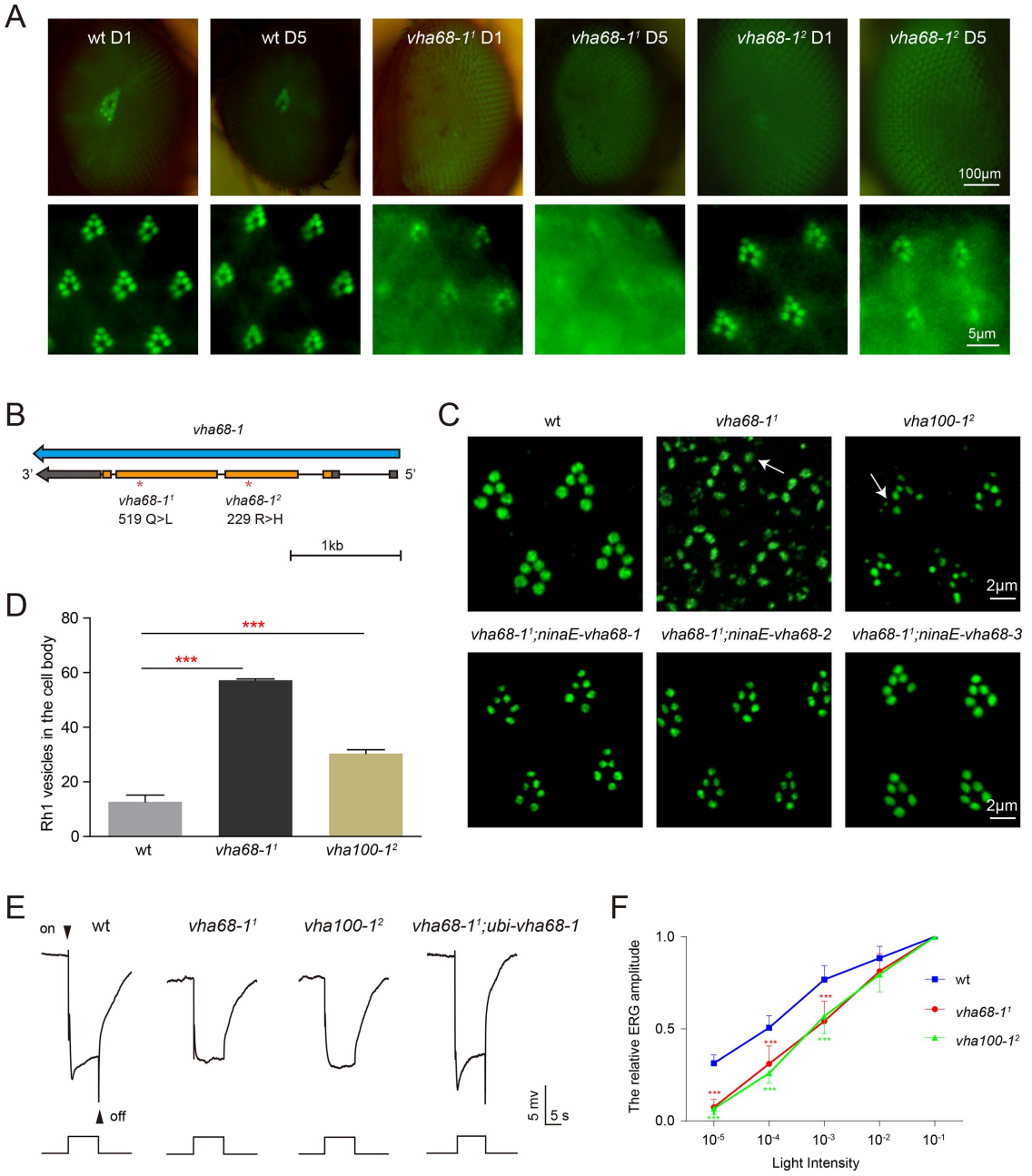

FIGURE 1: Rhodopsin mislocalization, defective visual transmission, and reduced light sensitivity in *vha68-1* mutants. (A) Isolation of the *vha68-1*^{1} and *vha68-1*^{2} mutations via a forward genetic screen. Rh1-GFP fluorescence was detected in the deep pseudopupil (top) and by corneal optical neutralization (bottom). Images from 1-d-old and 5-d-old wild-type (wt: *ey-flp rh1-GFP; FRT40A/GMR-hid CL FRT40A*), *vha68-1*^{1}(*ey-flp rh1-GFP;vha68-1*^{1} *FRT40A/GMR-hid CL FRT40A*), and *vha68-1*^{2} (*ey-flp rh1-GFP;vha68-1*^{2} *FRT40A/GMR-hid CL FRT40A*) flies are shown. Flies were raised in 12-h light/12-h dark cycles. (B) The *vha68-1* locus and mutations associated with the *vha68-1*^{1} and *vha68-1*^{2} alleles. (C) Rh1 accumulated in the cell body of both *vha68-1*^{1} and *vha100-1*^{2} (*ey-flp rh1-GFP;FRT82B vha100-1*^{2}*/FRT82B GMR-hid CL*) photoreceptor cells. Tangential resin-embedded retinal sections of compound eyes from ~1-d-old wt, *vha68-1*^{1}, *vha100-1*^{2}, *vha68-1*^{1}*;ninaE-vha68-1* (*ey-flp rh1-GFP; vha68-1*^{1} *FRT40A/GMR-hid CL FRT40A;ninaE-vha68-1/+*), *vha68-1*^{1}*;ninaE-vha68-2* (*ey-flp rh1-GFP; vha68-1*^{1} *FRT40A/GMR-hid CL FRT40A;ninaE-vha68-2/+*), and *vha68-1*^{1}*;ninaE-vha68-3* (*ey-flp rh1-GFP; vha68-1*^{1} *FRT40A/GMR-hid CL FRT40A;ninaE-vha68-3/+*) flies were labeled using anti-Rh1 antibodies. Rh1 vesicles are indicated by arrows in *vha68-1*^{1} and *vha100-1*^{2} cell bodies. (D) Quantification of Rh1 vesicles shown in C. Nine 20 × 20 μm areas from each section of three different eyes were quantified for each genotype. Error bars indicate SD; ***, $p < 0.001$ (Student's unpaired *t* test). (E) ERG recordings from 1-d-old wt, *vha68-1*^{1}, *vha100-1*^{2}, and *vha68-1*^{1}*;ubi-vha68-1* (*ey-flp rh1-GFP; vha68-1*^{1} *FRT40A/GMR-hid CL FRT40A;ubi-vha68-1/+*) flies. Flies were exposed to a 5-s pulse of orange light after 2 min of dark adaptation. On and off transients are indicated. (F) Reduced light sensitivity in *vha68-1*^{1} and *vha100-1*^{2} flies. ERG amplitudes at each intensity are normalized to ERG amplitudes at maximum light intensity (10^{-1}, ~300 lux). Error bars represent SD; significant differences were determined using the unpaired Student's *t* test ($n = 7$, ***, $p < 0.001$).

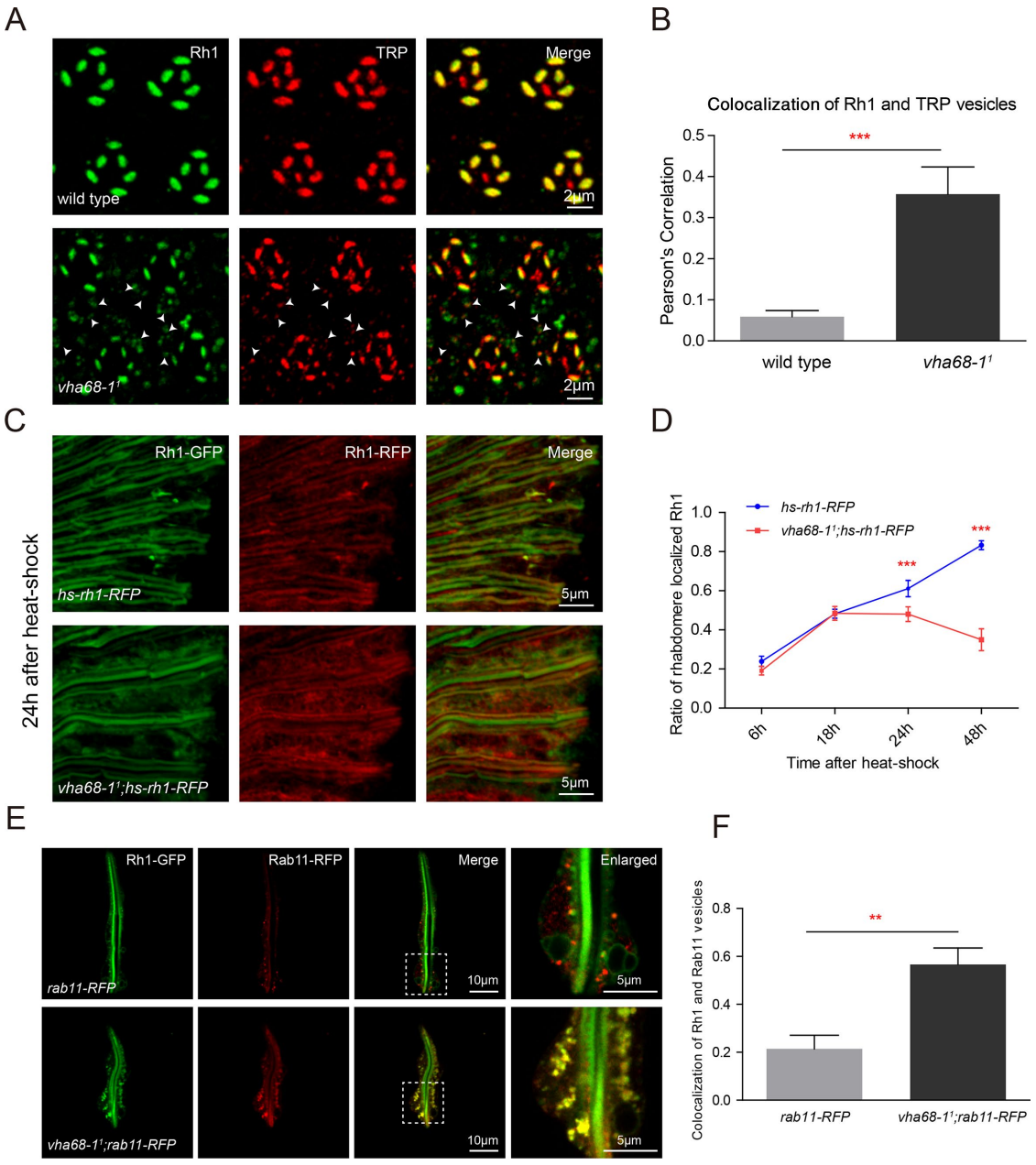

FIGURE 2: Vha68-1 is required for Rh1 maturation. (A) Tangential resin-embedded retinal sections from ~1-d-old wild-type and *vha68-1*[1] flies were labeled using antibodies against Rh1 (green) and TRP (red). Colocalized Rh1 and TRP vesicles are indicated by arrowheads in *vha68-1*[1] cell bodies. (B) Quantification of the Pearson's correlation between Rh1 and TRP vesicles. Images of retinas from six different flies for each genotype were used for quantification. Error bars represent SD; ***, $p < 0.001$ (Student's unpaired *t* test). (C) Cryostat sections of *hs-rh1-RFP* (*ey-flp rh1-GFP;hs-rh1-RFP/+*) and *vha68-1*[1]*;hs-rh1-RFP* (*ey-flp rh1-GFP;vha68-1*[1] *FRT40A/GMR-hid CL FRT40A; hs-rh1-RFP/+*) labeled using RFP antibodies are shown. Flies were heat shocked for 1 h and kept in the dark for 24 h. GFP fluorescence of Rh1-GFP was directly observed to indicate rhabdomeres. (D) Quantification of rhabdomere-localized, newly synthesized Rh1-RFP at indicated time points after a 1-h heat shock. Six different compound eye sections of each sample were quantified. Error bars indicate SD; ***, $p < 0.001$ (Student's unpaired *t* test). (E) Live confocal imaging of dissected ommatidia from *rab11-RFP* (*rh1-GFP;ninaE-rab11-RFP/+*) and *vha68-1*[1]*;rab11-RFP* (*ey-flp rh1-GFP;vha68-1*[1] *FRT40A/GMR-hid CL FRT40A;ninaE-rab11-RFP/+*) flies. Images with high magnification are shown in right panels. (F) Quantification of colocalization between Rh1 and Rab11 vesicles. At least 15 ommatidia from three compound eyes of each genotype were quantified. Error bars indicate SD; **, $p < 0.01$ (Student's unpaired *t* test).

(transient receptor potential), are synthesized in the ER and transported to rhabdomeric membranes. Rh1 is rapidly endocytosed in response to light, whereas TRP is stabilized in rhabdomeres through formation of a complex with INAD (Inactivation no afterpotential D) (Tsunoda *et al.*, 1997; Han *et al.*, 2007; Wang *et al.*, 2014b; Schopf and Huber, 2017). Thus, in our analysis of wild-type animals, TRP localized exclusively to the rhabdomere, whereas Rh1 was found in small, cytoplasmic exocytic vesicles (Figure 2A). To determine

whether anterograde or retrograde trafficking was affected in *vha68-1*^{1} flies, we used immunohistochemistry to assess Rh1 and TRP localization in *vha68-1*^{1} mutant retinas. We found that TRP protein also accumulated in the cell bodies of *vha68-1*^{1} photoreceptors, largely colocalizing with Rh1 (Figure 2, A and B). In contrast, rhabdomeric localization of INAD was not affected in *vha68-1*^{1} flies (Supplemental Figure S4A). We also measured the localization of Na^+K^+ATPase, which is a basolateral membrane protein in fly photoreceptors. Na^+K^+ATPase localized normally in the basolateral membrane and did not accumulate in the cytoplasm of *vha68-1*^{1} adult eyes (Supplemental Figure S4B). These data indicate that anterograde trafficking of membrane proteins, including Rh1 and TRP, was defective in *vha68-1*^{1}photoreceptor cells, but transport toward the basolateral membrane was not affected.

To further distinguish between Rh1 biosynthetic and endocytic processes, we introduced into *vha68-1*^{1} mutant flies a transgene in which red fluorescent protein (RFP)-tagged Rh1 is expressed under control of the heat-shock promoter (*hs-rh1-RFP*). We used this fly to perform a pulse–chase assay (Supplemental Figure S5A). Young flies were exposed to a 37°C heat shock for 1 h to induce Rh1-RFP expression and subsequently kept in the dark to avoid Rh1-GFP endocytosis. The trafficking of newly synthesized Rh1-RFP was measured at 6, 18, 24, and 48 h after the heat shock. In wild-type flies, newly synthesized Rh1 was primarily detected in the rhabdomere by 24 h (Figure 2C and Supplemental Figure S5, B–E), as has been reported (Rosenbaum *et al*., 2011). In *vha68-1*^{1} flies, however, there was significantly less rhabdomeric Rh1 at both 24- and 48-h time points compared with wild type (Figure 2, C and D, and Supplemental Figure S5, D and E), indicating that Rh1 anterograde trafficking was affected in *vha68-1*^{1} flies. Although the trafficking of newly synthesized Rh1-RFP could be visualized in cryostat sections, we found that Rh1 vesicles were poorly preserved in this system. Rh1 vesicles were lost in both wild-type and *vha68-1*^{1} flies. However, Rh1 vesicles could be directly observed in dissected ommatidia (Figure 2E) or by staining resin-embedded sections (Figures 1C and 2A).

To separate the Rh1 exocytic and endocytic processes, we introduced the temperature-sensitive allele of dynamin, namely *shi*^{ts1}, into *vha68-1*^{1}*;hs-Rh1-RFP* flies. Dynamin is required for Rh1 endocytosis upon light exposure (Alloway *et al*., 2000). Dynamin function is normal at the permissive temperature of 18°C but loses its function at elevated temperatures. Impaired dynamin function inhibits the endocytic process. Newly eclosed flies were exposed to a 37°C heat shock for 1 h and subsequently kept in the dark at 25°C. The trafficking of newly synthesized Rh1-RFP was measured at 24 h after the heat shock. In *vha68-1*^{1} flies, newly synthesized Rh1 was still less localized to the rhabdomere compared with wild type (Supplemental Figure S6, A and B). We also measured Rh1 vesicles in *vha68-1*^{1} *ninaE-Gal4;UAS-shi*^{ts1} flies. Rh1 vesicles still accumulated in *vha68-1*^{1} flies, even though the endocytotic pathway was blocked (Supplemental Figure S6C). These data indicate that Vha68-1 is required for Rh1 anterograde trafficking to the rhabdomere.

It has been reported that Rab11 functions in post-Golgi trafficking of Rh1 and TRP to rhabdomeric membranes of photoreceptors and that Rab11 may serve as a marker for the post-Golgi secretory pathway (Satoh *et al*., 2005). We therefore asked whether Rh1 accumulated in Rab11-positive vesicles in *vha68-1*^{1} mutant cells. We introduced *rab11-RFP* into *vha68-1*^{1} flies and dissected ommatidia for live imaging. Indeed Rh1 largely colocalized with Rab11 in *vha68-1*^{1} photoreceptor cells (Figure 2, E and F). These results suggest that Vha68-1 plays a role in the post-Golgi trafficking of rhodopsin to the apical rhabdomere membrane.

Vha68-1 is required for Rh1 deglycosylation

Because Vha68-1 is a subunit of the cytosolic V1 domain of V-ATPase, we asked whether the pH gradient of secreted vesicles was disrupted in *vha68-1*^{1} photoreceptors. For this analysis, we fused the secretory vesicle protein nSyb (neuronal Synaptobrevin) to a pH-sensitive version of GFP, called pHluorin, together with pH-insensitive mCherry (Koivusalo *et al*., 2010). The nSyb-mCherry-pHluorin reporter (hereafter referred to as nSyb-mp) was then expressed in photoreceptor cells using the *ninaE* promoter, and the subcellular localization of the reporter was measured. We performed colocalization analysis of Rh1 and the nSyb-mp reporter in the adult eye. Rh1 vesicles largely colocalized with nSyb vesicles, both in wild-type and *vha68-1*^{1} flies (Figure 3A).Vha100-1 localizes to presynaptic photoreceptor terminals in the lamina (Hiesinger *et al*., 2005). The nSyb-mp reporter colocalized with Vha100-1 in the synaptic terminals (Supplemental Figure S7A). Vha100-1 colocalized with multiple endosome markers in the lamina, including Rab5, Rab7, and Rab11, but colocalized less with the lysosome marker Lamp1 (Supplemental Figure S7B). Similarly, comprehensive colocalization analysis has revealed that Vha100-1 strongly colocalizes with early endosome markers and synaptic vesicles, but exhibits less colocalization with lysosomal markers (Williamson *et al*., 2010). These results indicate that the nSyb-mp reporter colocalizes with Rh1 vesicles in the retina and localizes to synaptic terminals in the lamina.

In wild-type flies, green fluorescence was barely detectable in dissected ommatidia, due to low pH. However, the pHluorin signal was readily detected in *vha68-1*^{1} ommatidia, with the pHluorin/mCherry fluorescence ratio approaching 1 (Figure 3, B and C). These results demonstrate that pH levels were increased in *vha68-1*^{1} secretory vesicles.

During biosynthesis, Rh1 is transiently glycosylated at Asn20 within the extracellular N-terminal region. This modification is removed as it is transported from the ER to the rhabdomere (O'Tousa, 1992; Webel *et al*., 2000; Rosenbaum *et al*., 2014). As several glycosyl hydrolase enzymes involved in glycoprotein deglycosylation are present in the exocytic vesicles (Nilsson *et al*., 2009; Fisher and Ungar, 2016), we asked whether Rh1 deglycosylation was disrupted in V-ATPase mutants, which exhibit loss of acidification. We observed an increase in the molecular weight (MW) of Rh1 in both *vha68-1*^{1} and *vha100-1*^{2} flies (Figure 3D and Supplemental Figure S3B). After extracts were digested with two glycosidases, endoglycosidase H (Endo H) and peptide N-glycosidase F (PNGase F), Rh1 from *vha68-1*^{1} or *vha100-1*^{2} animals was reduced to wild-type size (Figure 3D). Moreover, Rh1 deglycosylation defects were rescued by expressing *vha68-1*, *vha68-2*, or *vha68-3* in *vha68-1*^{1} mutants (Figure 3E).

We next sought to determine which step in the deglycosylation process involves Vha68-1. NinaA is an ER chaperone for Rh1, and immature Rh1 with an untrimmed N-linked glycosylation is retained in the ER of *ninaA* mutants (Colley *et al*., 1991). As expected, Rh1 protein was smaller in *vha68-1*^{1} than in *ninaA*^{2} flies, indicating that Vha68-1 functions downstream of the ER (Figure 3F). *Drosophila* metallophosphoesterase (dMppe) is required for Rh1 deglycosylation in the Golgi, and Rh1 MW was slightly greater in *dmppe*^{e02905} mutants than in *vha68-1*^{1} flies (Figure 3F) (Cao *et al*., 2011). We next generated *vha68-1*^{1} *dmppe*^{e02905} double mutants and found that Rh1 MW in the double mutants was indistinguishable from that measured in *dmppe*^{e02905} flies (Figure 3F). This indicates that Vha68-1 functions downstream of the Golgi in Rh1 deglycosylation. Although it has been reported that glycosyl hydrolases for removal of the remaining mannose residues and the two core GlcNAc residues retain deglycosylation activity at neutral

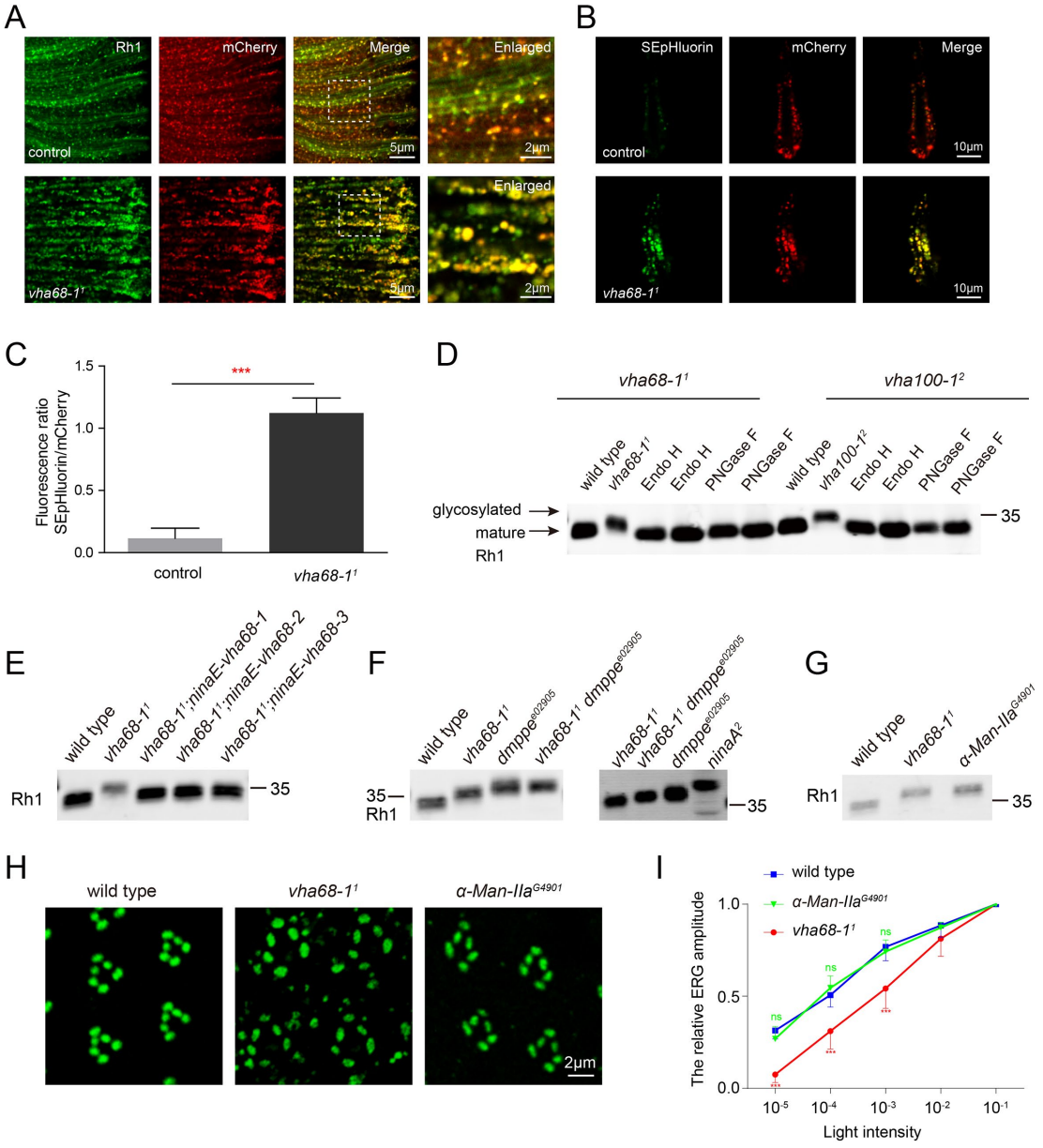

FIGURE 3: Vha68-1 is required for Rh1 deglycosylation and pH homeostasis of secretory vesicles. (A) Rh1 vesicles and nSyb secretory vesicles largely colocalized. Eyes from control (*ninaE-nSyb-mCherry-pHluorin/+*) and *vha68-1*^{1} (*ey-flp; vha68-1*^{1} *FRT40A/GMR-hid CL FRT40A; ninaE-nSyb-mCherry-pHluorin/+*) flies expressing nSyb-mCherry-pHluorin were labeled with antibodies against Rh1 (green) and RFP (red). Images with high magnification are shown in right panels. (B) Secretory vesicle pH was increased in *vha68-1*^{1} photoreceptors. Live confocal imaging of dissected ommatidia from control and *vha68-1*^{1} flies expressing nSyb-mCherry-pHluorin. The pHluorin fluorescence was brighter in *vha68-1*^{1} flies compared with controls, which indicates an increase in pH. (C) Quantification of fluorescence ratios in control and *vha68-1*^{1} flies. Four eyes from different flies and 20 ommatidia from each eye were quantified. Error bars represent SD; ***, $p < 0.001$ (Student's unpaired *t* test). (D) The increase in Rh1 MW is due to a failure of deglycosylation. Head extracts prepared from 1-d-old *vha68-1*^{1} or *vha100-1*^{2} flies were digested with Endo H or PNGase F at 37°C for 4 h before being labeled with antibodies against Rh1. (E) Rh1 MW was reverted to wild type upon expression of *vha68-1*, *vha68-2*, or *vha68-3* in photoreceptor cells. Western blot analysis of head extracts from 1-d-old wild-type, *vha68-1*^{1}, *vha68-1*^{1}*;ninaE-vha68-1*, *vha68-1*^{1}*;ninaE-vha68-2*, and *vha68-1*^{1}*;ninaE-vha68-3* flies that were labeled with antibodies against Rh1. One-day-old flies were used. (F) Vha68-1 functions downstream of dMPPE. Head extracts were prepared from 1-d-old wild-type, *vha68-1*^{1}, *dmppe*^{e02905}, *vha68-1*^{1} *dmppe*^{e02905}(*ey-flp rh1-GFP;vha68-1*^{1} *FRT40A dmppe*^{e02905}*/ GMR-hid CL FRT40A dmppe*^{e02905}), and *ninaA*^{2}flies and labeled with antibodies against Rh1. (G) Similar Rh1 MW in *vha68-1*^{1} and α*-Man-IIa*^{G4901} flies. Head extracts were prepared from 1-d-old flies and labeled with antibodies against Rh1. (H) Tangential resin-embedded sections of compound eyes from ~1-d-old wild-type, *vha68-1*^{1}, and α*-Man-IIa*^{G4901} flies were labeled using antibodies against Rh1 (green). Rh1 vesicles did not accumulate in α*-Man-IIa*^{G4901} flies, which showed deglycosylation defects. (I) Light-sensitivity analysis of ~1 d posteclosion flies. ERG amplitudes at each intensity are normalized to ERG amplitudes at maximum light intensity (10^{-1}, ~300 lux). $n = 7$; data are presented as mean ± SD; ***, $p < 0.001$ (Student's unpaired *t* test).

pH (Leonard *et al.*, 2006; Rosenbaum *et al.*, 2014), a single large Rh1 band was detected in both *vha68-1*^{1} and *vha100-1*^{1} mutants, indicating that these glycosyl hydrolases failed to function in high pH. Therefore, our data suggest that the final steps of rhodopsin deglycosylation occur in post-Golgi vesicles and that low pH is required for proper functioning of relevant glycosyl hydrolases.

In the mutant genes *ninaA* and *santa maria* (*scavenger receptor acting in neural tissue and majority of rhodopsin is absent*), which encode a peptidyl-prolyl *cis-trans* isomerase and a class B scavenger receptor, respectively, Rh1 remains fully glycosylated and accumulates in the ER, suggesting deglycosylation of newly synthesized rhodopsin may be essential for its rapid transport to the rhabdomere (Colley *et al.*, 1991; Wang *et al.*, 2007). However, incomplete deglycosylation of Rh1 within the Golgi of *dmppe* mutants did not affect Rh1 localization (Cao *et al.*, 2011). To establish the relationship between Rh1 deglycosylation defects and the Rh1 accumulation in vesicles of *vha68-1*^{1} mutants, we used a mutation in the gene α-*Man-IIa*, which mediates Rh1 deglycosylation (Cao *et al.*, 2011; Rosenbaum *et al.*, 2014). Although, the size of Rh1 was similar between *vha68-1*^{1} and α-*Man-IIa*^{G4901} flies, Rh1 did not accumulate in vesicles in α-*Man-IIa*^{G4901} flies, and the light sensitivity of α-*Man-IIa* mutants was indistinguishable from that of wild-type flies (Figure 3, G–I). Moreover, TRP, which is likely not subjected to N-glycosylation modification, was also mislocalized in *vha68-1*^{1} cells. In addition, Rh1 vesicles still accumulated in *vha68-1*^{1} *dmppe*^{e02905} double mutants (Supplemental Figure S8A). Although dMppe functions upstream of Vha68-1 in the Rh1 deglycosylation process, dMppe could not suppress Rh1 accumulation phenotypes in *vha68-1*^{1} flies. These results suggest that the deglycosylation of newly synthesized rhodopsin in the post-Golgi secretory pathway is not required for its trafficking to the rhabdomere.

To investigate the relationship between Rh1 post-Golgi trafficking and increased vesicle pH, we exploited a single amino acid mutation, R755A, that specifically disrupts the proton translocation function of V100 (Williamson *et al.*, 2010). *v100*^{R755A}*-GFP* was expressed in the *vha100-1*^{2} mutant background using the *ninaE* promoter. This acidification-defective form of V100 could not rescue Rh1 vesicle accumulation or Rh1 deglycosylation phenotypes (Supplemental Figure S8, B and C). These results indicate that V-ATPase is required to maintain pH in Rh1 secretory vesicles during its trafficking to the rhabdomere.

Mutations in *vha68-1* lead to light-independent retinal degeneration

Because Rh1 showed unusual cellular localization and abnormal posttranslational modifications, we set out to determine whether photoreceptor integrity depends on Vha68-1. Wild-type ommatidia consistently exhibited seven intact rhabdomeres, regardless of age and light/dark conditions (Figure 4A). However, *vha68-1*^{1} flies displayed light-independent loss of photoreceptor cells and rhabdomeres. Twenty-day-old *vha68-1*^{1} flies exhibited a complete loss of rhabdomeres within R1-R6 cells when reared either in a light/dark cycle or constant darkness. Moreover, many vesicles accumulated in *vha68-1*^{1} cell bodies, even shortly after eclosion under both dark and light conditions, reflecting an accumulation of secretory vesicles (Figure 4, B and C). A cross-section of wild-type ommatidium contains seven photoreceptors, organized in a stereotypical pattern (Figure 4D). Cell-death and vesicle-accumulation phenotypes in *vha68-1*^{1} flies were completely rescued by expressing *vha68-1*, *vha68-2*, or *vha68-3* (Figure 4E). These results demonstrate that Vha68-1 is required for photoreceptor cell survival.

DISCUSSION

In addition to functioning in vesicular acidification, V-ATPase is also involved in trafficking and processing of plasma membrane receptors, such as receptors in the Wnt and Notch signaling pathways in both vertebrates and invertebrates (Yan *et al.*, 2009; Buechling *et al.*, 2010; Cruciat *et al.*, 2010; Hermle *et al.*, 2010; Vaccari *et al.*, 2010). Here, we isolated mutations in the V1 component subunit, Vha68-1. In these mutants, maturation of the photon receptor, rhodopsin, was disrupted, impairing light sensitivity of photoreceptors. Rhodopsin accumulated in vesicles in these mutant photoreceptors, but this accumulation did not result from disruption of endocytic trafficking or degradation of the receptor. We base this conclusion on four results. First, The TRP channel accumulated together with rhodopsin in photoreceptor cell bodies, even though TRP is not normally subjected to high levels of endocytosis. In contrast, INAD, which forms a complex with TRP in rhabdomeres, still localized to the rhabdomere in *vha68-1* mutant cells, suggesting that mislocalization of TRP occurred upstream of formation of the signalplex with INAD (Li and Montell, 2000). Second, a pulse–chase assay demonstrated that rhodopsin maturation was dramatically slower in *vha68-1* mutants compared with wild-type controls. Rh1 vesicles still accumulated in *vha68-1*^{1} flies in the *shi*^{ts1} background, which blocks the endocytotic pathway. Third, cytosolic rhodopsin largely colocalized with Rab11, a marker of the post-Golgi secretory pathway (Satoh *et al.*, 2005). Finally, loss of Vha68-1 led to severe, light-independent retinal degeneration, whereas retinal degeneration in mutations that affect retrograde trafficking of endocytic rhodopsin require light to activate the endocytic event (Xu *et al.*, 2004; Chinchore *et al.*, 2009; Xu and Wang, 2016). We therefore propose a model in which Vha68-1 functions in post-Golgi secretory vesicles to deglycosylate and transport Rh1 to the apical rhabdomere membrane (Figure 5).

Direct involvement of the V0 component in membrane fusion, independent of the V1 component, has been demonstrated in worm, fly, zebrafish, and mouse models (Peters *et al.*, 2001; Baars *et al.*, 2007; Stroupe *et al.*, 2009; Strasser *et al.*, 2011; Sreelatha *et al.*, 2015). However, a role for the V0 domain in homotypic fusion is controversial, as vacuole acidification may instead be the mechanism by which V-ATPase affects this process (Ungermann *et al.*, 1999; Coonrod *et al.*, 2013). In flies, mutations in the largest V0 component, *vha100-1*, lead to synaptic vesicle accumulation and loss of visual transmission in synaptic terminals (Hiesinger *et al.*, 2005). Although these data suggest that Vha100-1 and perhaps other V0 components mediate the release of synaptic vesicles, their potential role in the acidification of synaptic vesicles must also be taken into account. Recently, a mutation in the B subunit of V1 was isolated in *C. elegans*. This mutant exhibits defects in acetylcholine neurotransmission, suggesting a crucial role of the V1 component in membrane fusion (Ernstrom *et al.*, 2012). Here, we identified a mutation in the A1 subunit of the V1 component, and mutations in both *vha68-1* and *vha100-1* disrupted visual transmission and displayed Rh1 trafficking defects, suggesting that V1 and V0 may both play vital roles in membrane fusion. It has been reported that V-ATPase is also important for sorting proteins in the secretory pathway, as disruption of V-ATPase activity causes cytoplasmic accumulation of plasma membrane proteins and secretory granules (Sobota *et al.*, 2009; Huang and Chang, 2011). Nevertheless, our data support a key role of V-ATPase in anterograde trafficking of membrane proteins.

Genetic mutations affecting V-ATPase have been identified in several human autosomal-recessive disorders. In particular, mutations in the V0 component subunit *ATP6V0A2*, the counterpart of fly *vha100*, cause symptoms of cutis laxa, a condition characterized by

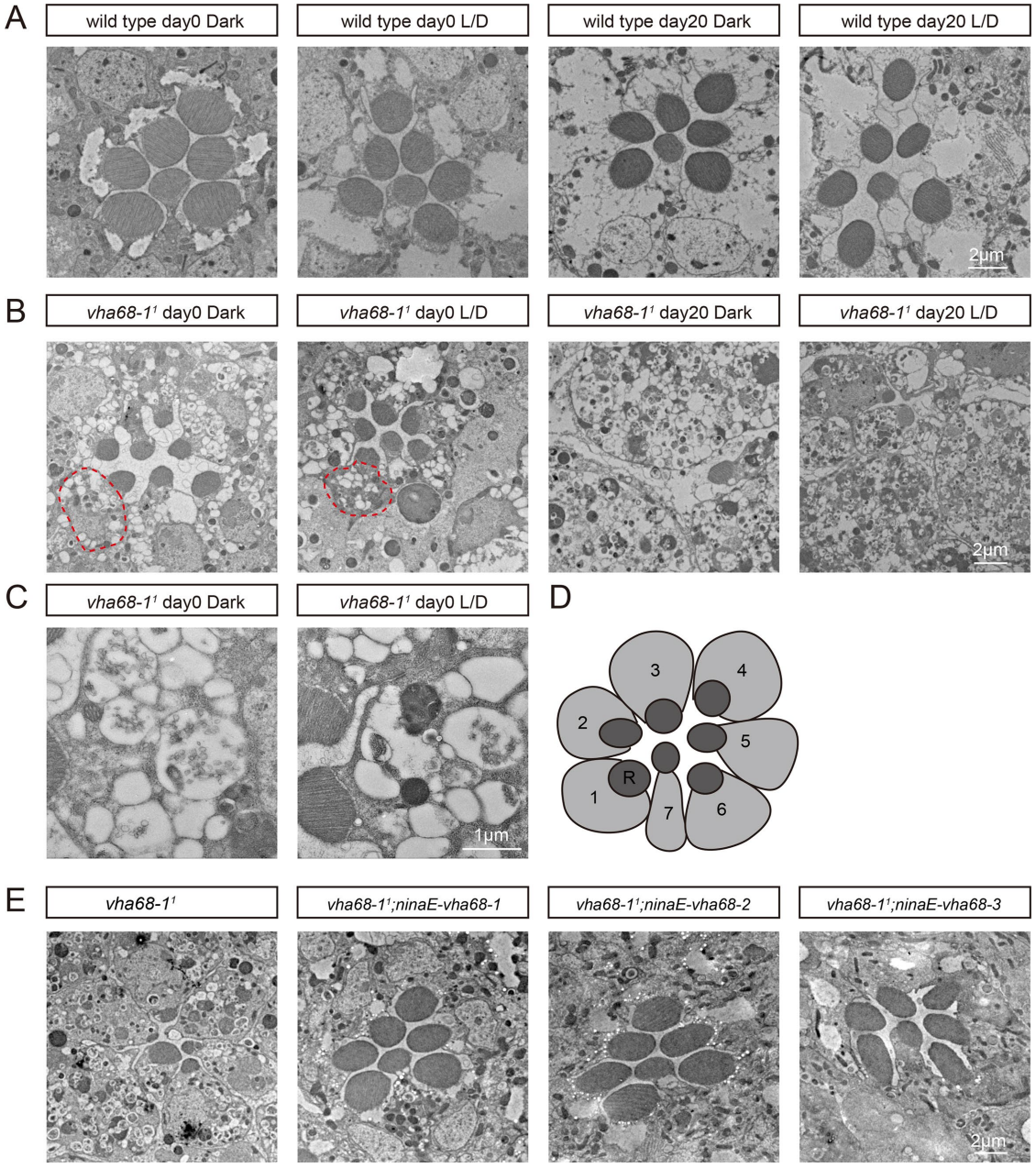

FIGURE 4: Light-independent retinal degeneration and massive vesicle accumulation in *vha68-1*^{1} photoreceptors. (A–C) Transmission electron microscopy images of representative ommatidia are shown. Sections were obtained from wild-type (A) or *vha68-1*^{1} (B) flies, which were raised in the dark or in 12-h light/12-h dark (L/D) cycles for the indicated time points. Red circles indicate cell bodies filled with vesicles. (C) Vesicles accumulated in a single photoreceptor cell of *vha68-1*^{1} flies raised in the dark or in 12-h light/12-h dark (L/D) cycles at day 0. (D) Cartoon picture illustrates photoreceptor cells in a single ommatidium in the distal region. Seven photoreceptor cells (1–7) are marked and shown. R, rhabdomere. (E) Suppression of retinal degeneration in *vha68-1*^{1} mutants by *ninaE-vha68-1*, *ninaE-vha68-2*, or *ninaE-vha68-3*. All flies were raised for 10 d under 12-h light/12-h dark cycles.

disrupted vesicular trafficking, abnormal glycosylation of serum proteins, intracellular accumulation of tropoelastin, and reduced levels of mature elastin in the extracellular matrix (Kornak *et al.*, 2008; Hucthagowder *et al.*, 2009). Recently, mutations in ATP6V1A, the counterpart of fly Vha68, have also been implicated in cutis laxa disorders, affecting protein glycosylation, Golgi trafficking, and extracellular matrix homeostasis (Van Damme *et al.*, 2017). As mutations in fly *vha68-1* affect the deglycosylation and post-Golgi trafficking of rhodopsin, resulting in retinal degeneration, this system represents a conserved model for studying diseases associated with defective V-ATPase. Thus, these genetic reagents provide opportunities for exploiting this model organism to identify genetic and/or pharmacological suppressors of V-ATPase mutants.

MATERIALS AND METHODS

Fly stocks

The following stocks were obtained from the Bloomington Stock Center: 1) y^{d2} w^{1118}; *P[neoFRT] 82B Vha100-1*^{2}*/TM3, Sb*^{1}, 2) *w*; ninaA*^{2}, 3) w^{1118}; *PEP* α*-Man-IIa*^{G4901}, 4) *M(vas-int.Dm)ZH-2A;M(3xP3-RFP.attP)ZH-86Fb*, 5) w^{1118}, 6) *w*; P[UAS-shi*^{ts1}*.K]3*. The *PBac*

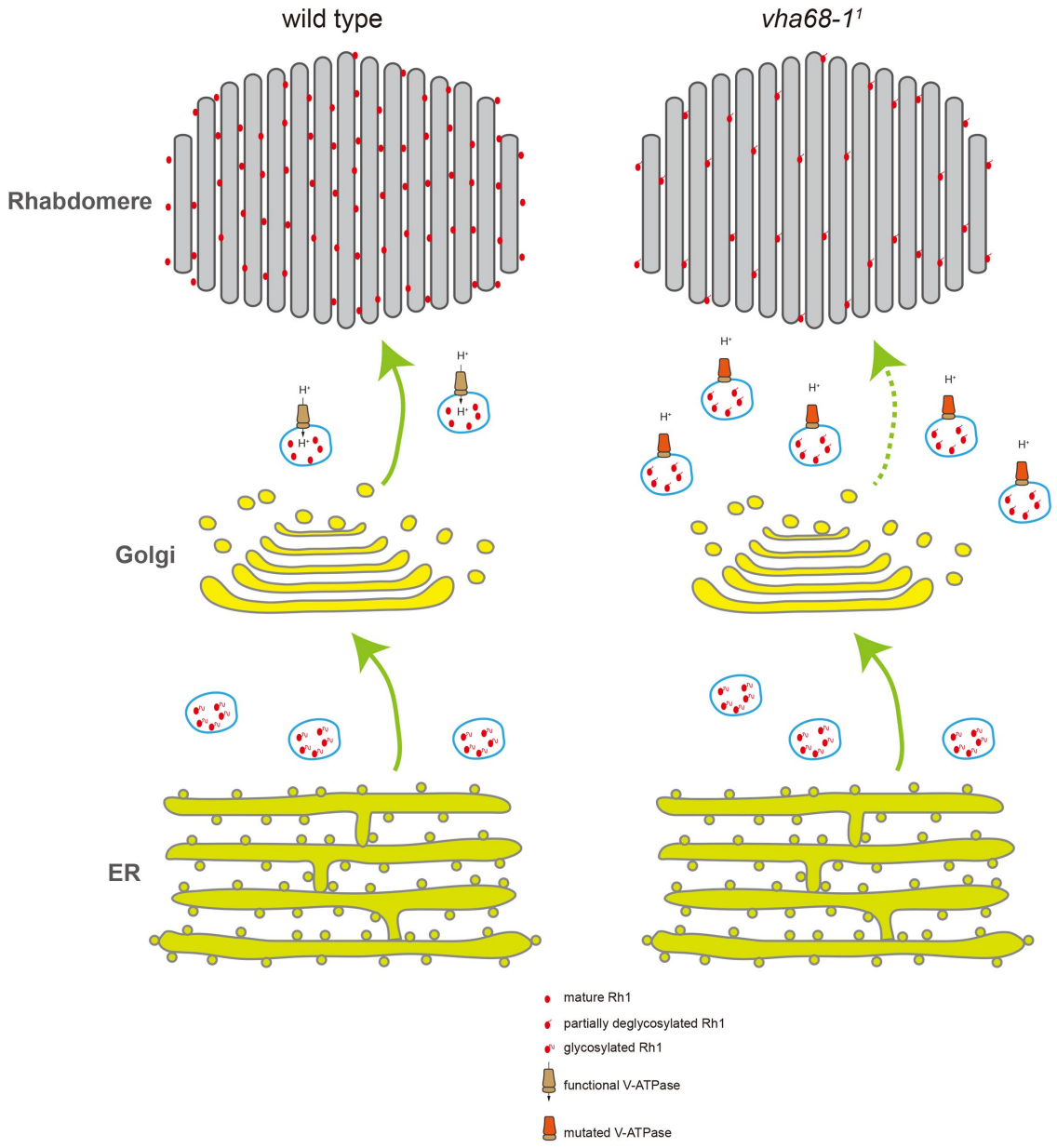

FIGURE 5: Model of Vha68-1 function in Rh1 trafficking. In wild-type flies, Rh1 is synthesized in the ER and undergoes N-glycosylation. Oligosaccharides are sequentially removed in the Golgi and secretory vesicles before mature Rh1 is delivered to the rhabdomere. In *vha68-1*^{1} mutant flies, post-Golgi secretory vesicles fail to maintain low pH level because of V-ATPase malfunction. As a result, Rh1 is not fully deglycosylated, accumulating in secretory vesicles within the photoreceptor cell body. Levels of functional Rh1 are therefore reduced in the rhabdomere.

Mppe^{e02905} flies were obtained from J. Han (Institute of Life Science, Southeast University, China). The *ninaE-rab5-rfp*, *ninaE-rab7-rfp*, *ninaE-rab11-rfp*, *ninaE-lamp1-rfp*, *ey-flp ninaE-Rh1-GFP;FRT40A*, *ey-flp ninaE-Rh1-GFP;GMR-hid CL FRT40A/Cyo*, and *ey-flp ninaE-Rh1-GFP;FRT82B GMR-hid CL/TM3* flies were maintained in the laboratory of T.W. Flies were maintained in 12-h light/12-h dark cycles with 2000 lux illumination at 25°C, unless different conditions are described in the text.

EMS mutagenesis

The second chromosome of *ey-flp,ninaE-Rh1-GFP;FTR40A* flies was isogenized, and young male flies were fed 25 mM EMS (Sigma, St. Louis, MO) in 2% sucrose for 8 h. Mutagenized flies were mated immediately to *ey-flp ninaE-Rh1-GFP;GMR-hid CL FRT40A/Cyo* flies (Supplemental Figure S1). F1 progeny were screened by performing fluorescence DPP assays at days 1 and 5 following eclosion. Approximately 10,000 F1 flies were screened.

Generation of transgenic flies

The *vha68-1*, *vha68-2*, *vha68-3*, *vha100-1*, and *nSyb* cDNAs were amplified from the cDNA clones GH21132, RE30552, AT09773, LD21248, and GH04664, respectively, which were obtained from the *Drosophila* Genomic Resource Center. For expression of *vha68-1*, *vha68-2*, and *vha68-3* cDNAs under control of the *ninaE* promoter, the cDNAs were subcloned into the *pninaE-attB* vector between the *Not*I and *Xba*I sites (Xu and Wang, 2016). The *vha100-1* cDNA was

subcloned into the *pIB-c-GFP* or *pIB-c-myc* vector between the *Eco*RI and *Not*I sites. The mutant form *v100^{R755A}* was obtained using site-directed mutagenesis. The fragment *v100-GFP*, *v100^{R755A}-GFP*, or *v100-myc* was separately subcloned into the *pninaE-attB* vector between the *Eco*RI and *Xba*I sites. The *nSyb* cDNA was subcloned into the *pIB-mcherry-pHluorin* vector between the *Hin*dIII and *Eco*RI sites. The *mcherry-pHluorin* vector was a gift from S. Grinstein (Department of Biochemistry, University of Toronto, Canada) (Addgene plasmid #32001). The *nSyb-mcherry-pHluorin* fragment was subcloned into the *pninaE-attB* vector. These constructs were injected into *M(vas-int.Dm)ZH-2A;M(3xP3-RFP.attP)ZH-86Fb* embryos, and transformants were identified on the basis of eye color (Bischof *et al.*, 2007). The *3xP3-RFP* marker was eliminated by crossing to a Cre-expressing line.

For expression of RFP-labeled Rh1 under control of the *heat-shock* (*hs*) promoter, an RFP tag was added to the C terminus of the *rh1* cDNA sequence and subsequently subcloned into the *pCaspeR-hs* vector between the *Not*I and *Xba*I sites. The construct was injected into *w^{1118}* embryos, and transformants were identified on the basis of eye color.

Fly imaging and optical neutralization assay

Flies were anaesthetized on a CO_2 pad, and fluorescence DPP images were taken with a Leica M165 FC Fluorescence Stereo Microscope (Leica, Wetzlar, Germany). For the optical neutralization assay, fly heads were immersed in mineral oil with antennae facing up. Samples were observed using a Nikon Ni-U fluorescence microscope equipped with a CFI Plan Fluor 40× objective (Nikon, Tokyo, Japan).

Western blotting and glycosidase treatment of Rh1

For Western blotting, fly heads were homogenized in SDS sample buffer with a pellet pestle (Fisher, Pittsburgh, PA). Proteins were then fractionated by SDS–PAGE and transferred to Immobilon-FL transfer membranes (Millipore, Carrigtohill, Ireland) in Tris-glycine buffer. The blots were probed with primary antibodies against Rh1 (mouse, 1:2000; Developmental Studies Hybridoma Bank, Iowa City, IA) or INAD (rabbit, 1:2000, Wang *et al.*, 2008), followed by IRDye 680 goat anti-mouse immunoglobulin G (IgG) or IRDye 800 goat anti-rat IgG (Li-Cor, Lincoln, NE) as secondary antibodies. Signals were detected using an Odyssey infrared imaging system (Li-Cor, Lincoln, NE).

All reagents for the Endo H and PNGase F digestions were obtained from New England Biolabs (NEB, Ipswich, MA). Twenty fly heads were collected and homogenized in glycoprotein denaturing buffer (1% SDS, 80 mM dithiothreitol). Homogenates were incubated for 4 h at 22°C and centrifuged to collect the supernatant. Digest reactions were processed according to manufacturer's instructions with slight modification. Specifically, the reactions were incubated for 4 h at 37°C. All samples were solubilized in SDS loading buffer to equal volumes for Western blot analysis.

ERG recordings

ERG recordings were performed as previously described (Wang *et al.*, 2008). Two glass microelectrodes filled with Ringer's solution were inserted into small drops of electrode cream (Parker Laboratories, Fairfield, NJ) that were placed onto the surface of the compound eye and the thorax. A Newport light projector (model 765) was used for stimulation. ERG signals were amplified with a Warner electrometer IE-210 and recorded with a MacLab/4s analogue-to-digital converter and the clampelx v. 10.2 program (Warner Instruments, Hamden, CT). All recordings were carried out at room temperature.

Immunohistochemistry

Hemisected fly heads were fixed with 4% paraformaldehyde (PFA) in phosphate-buffered saline (PBS) and embedded in LR White resin as described (Wang *et al.*, 2005). Cross-sections (0.5 µm) of compound eyes were cut through the distal region of the retina, which included the R7 cells. Sections were incubated with primary antibodies against Rh1 (mouse monoclonal 4C5, 1:200; Developmental Studies Hybridoma Bank, Iowa City, IA), TRP (rabbit, 1:200; Wang *et al.*, 2008), or INAD (rabbit, 1:200; Wang *et al.*, 2008) at room temperature for 1 h. Secondary antibodies against mouse or rabbit IgG labeled with Alexa Fluor 488 or Alexa Fluor 568, respectively, were used (1:400, Invitrogen, Waltham, MA). Images were captured with a Nikon A1-R confocal microscope (Nikon, Tokyo, Japan). Acquired images were processed using Photoshop CS6 and ImageJ (National Institutes of Health, Bethesda, MD). For measurement of the accumulation of Rh1 vesicles in cell bodies, sections from three different eyes and three 20 × 20 µm regions of each retina were quantified. The Pearson's correlation as a measure of colocalization between Rh1 and TRP vesicles was calculated using the Volocity software (PerkinElmer, Waltham, MA).

For the Rh1 heat-pulse assay and Vha100-1 colocalization analyses, fly heads were collected at indicated time points and fixed in 4% PFA in PBS (pH 7.4) for 1 h on ice. After three washes in PBS, heads were infiltrated with 12% sucrose overnight at 4°C. The next day, samples were submerged in optimal cutting temperature (Sakura, Torrance, CA) and sectioned at 10-µm thickness using a Leica CM1950 cryostat (Leica). Cryosections were incubated in 2% PFA in PBS for 10 min and then incubated with primary antibodies against RFP (rat, 1:200, Chromotek, Planegg, Germany), GFP (mouse monoclonal 12A6, 1:50; Developmental Studies Hybridoma Bank, Iowa City, IA) or Myc (rabbit, 1:200; Santa Cruz Biotechnology, Dallas, TX). Secondary antibodies against rat, mouse, or rabbit IgG labeled with Alexa Fluor 488, Alexa Fluor 568, or Alexa Fluor 647 were used (1:400; Invitrogen, Waltham, MA). Images were captured with a Nikon A1-R confocal microscope (Nikon, Tokyo, Japan). Acquired images were processed using Photoshop CS6 and NIS-Elements AR. The relative amount of Rh1-RFP present in the rhabdomere (R) was calculated using the formula R = Ir/Ib, where Ir and Ib are fluorescence intensities in the rhabdomeres and cell bodies, respectively.

Single ommatidium observation

Ommatidia from 1-d-old flies were dissected in Schneider's *Drosophila* medium (Invitrogen, Waltham, MA) as described (Xu *et al.*, 2004). Images were taken within 30 min under a Nikon A1-R confocal microscope (Nikon, Tokyo, Japan). The percentage of colocalization of Rh1 and Rab11 vesicles was calculated using the software Imaris X64 v. 7.4.2 (Bitplane, Zurich, Swizerland). Briefly, Rh1-positive and Rab11-positive vesicles were marked by red and green dots, respectively. The percentage of Rab11-positive Rh1 vesicles was calculated by the ratio of double-labeled dots to total red dots.

The SEpHluorin and mCherry fluorescence intensities of ommatidia were measured using ImageJ. The fluorescence ratios were calculated by quantifying four eyes from different flies; 20 ommatidia from each eye were used.

Transmission electron microscopy

Adult fly heads were dissected, fixed, dehydrated, and embedded in LR White resin (Ted Pella, Redding, CA) as previously described (Xu and Wang, 2016). Thin sections (80 nm) prepared at a depth of 30–40 µm were stained with uranyl acetate and lead

citrate (Sigma, St. Louis, MO) and examined using a FEI Tecnai Spirit Twin transmission electron microscope (FEI, Hillsboro, OR).

ACKNOWLEDGMENTS

We thank the Bloomington Stock Center, the *Drosophila* Genomic Resource Center, the Developmental Studies Hybridoma Bank, and H. Bellen, N. Colley, C. Montell, and J. Han for stocks and reagents. We thank Y. Wang and X. Liu for assistance with fly injections. We thank Ping Wu from the Imaging Facility of the National Center for Protein Science in Beijing for assistance with microscopy. We thank John Snyder for helpful discussions in preparing the article and D. O'Keefe for comments on the article. This work was supported by a grant from the National Natural Science Foundation of China (81670891) and by a "973" grant (2014CB849700) from the Chinese Ministry of Science (awarded to T.W.).

REFERENCES

Allan AK, Du J, Davies SA, Dow JAT (2005). Genome-wide survey of V-ATPase genes in *Drosophila* reveals a conserved renal phenotype for lethal alleles. Physiol Genomics 22, 128.

Alloway PG, Howard L, Dolph PJ (2000). The formation of stable rhodopsin-arrestin complexes induces apoptosis and photoreceptor cell degeneration. Neuron 28, 129–138.

Baars TL, Petri S, Peters C, Mayer A (2007). Role of the V-ATPase in regulation of the vacuolar fission fusion equilibrium. Mol Biol Cell 18, 3873–3882.

Bayer MJ, Reese C, Buhler S, Peters C, Mayer A (2003). Vacuole membrane fusion: V0 functions after *trans*-SNARE pairing and is coupled to the Ca^{2+}-releasing channel. J Cell Biol 162, 211–222.

Bischof J, Maeda RK, Hediger M, Karch F, Basler K (2007). An optimized transgenesis system for *Drosophila* using germ-line-specific phiC31 integrases. Proc Natl Acad Sci USA 104, 3312–3317.

Buechling T, Bartscherer K, Ohkawara B, Chaudhary V, Spirohn K, Niehrs C, Boutros M (2010). Wnt/Frizzled signaling requires dPRR, the *Drosophila* homolog of the prorenin receptor. Curr Biol 20, 1263–1268.

Cao J, Li Y, Xia W, Reddig K, Hu W, Xie W, Li HS, Han J (2011). A *Drosophila* metallophosphoesterase mediates deglycosylation of rhodopsin. EMBO J 30, 3701–3713.

Chinchore Y, Mitra A, Dolph PJ (2009). Accumulation of rhodopsin in late endosomes triggers photoreceptor cell degeneration. PLoS Genet 5, e1000377.

Colley NJ, Baker EK, Stamnes MA, Zuker CS (1991). The cyclophilin homolog ninaA is required in the secretory pathway. Cell 67, 255–263.

Colley NJ, Cassill JA, Baker EK, Zuker CS (1995). Defective intracellular transport is the molecular basis of rhodopsin-dependent dominant retinal degeneration. Proc Natl Acad Sci USA 92, 3070–3074.

Coonrod EM, Graham LA, Carpp LN, Carr TM, Stirrat L, Bowers K, Bryant NJ, Stevens TH (2013). Homotypic vacuole fusion in yeast requires organelle acidification and not the V-ATPase membrane domain. Dev Cell 27, 462–468.

Cotter K, Stransky L, McGuire C, Forgac M (2015). Recent insights into the structure, regulation, and function of the V-ATPases. Trends Biochem Sci 40, 611–622.

Cruciat CM, Ohkawara B, Acebron SP, Karaulanov E, Reinhard C, Ingelfinger D, Boutros M, Niehrs C (2010). Requirement of prorenin receptor and vacuolar H^+-ATPase-mediated acidification for Wnt signaling. Science 327, 459–463.

Ernstrom GG, Weimer R, Pawar DR, Watanabe S, Hobson RJ, Greenstein D, Jorgensen EM (2012). V-ATPase V1 sector is required for corpse clearance and neurotransmission in *Caenorhabditis elegans*. Genetics 191, 461–475.

Fisher P, Ungar D (2016). Bridging the gap between glycosylation and vesicle traffic. Front Cell Dev Biol 4, 15.

Forgac M (2007). Vacuolar ATPases: rotary proton pumps in physiology and pathophysiology. Nat Rev Mol Cell Biol 8, 917–929.

Haberman A, Williamson WR, Epstein D, Wang D, Rina S, Meinertzhagen IA, Hiesinger PR (2012). The synaptic vesicle SNARE neuronal synaptobrevin promotes endolysosomal degradation and prevents neurodegeneration. J Cell Biol 196, 261–276.

Han J, Reddig K, Li HS (2007). Prolonged G(q) activity triggers fly rhodopsin endocytosis and degradation, and reduces photoreceptor sensitivity. EMBO J 26, 4966–4973.

Hermle T, Saltukoglu D, Grunewald J, Walz G, Simons M (2010). Regulation of Frizzled-dependent planar polarity signaling by a V-ATPase subunit. Curr Biol 20, 1269–1276.

Hiesinger PR, Fayyazuddin A, Mehta SQ, Rosenmund T, Schulze KL, Zhai RG, Verstreken P, Cao Y, Zhou Y, Kunz J, Bellen HJ (2005). The v-ATPase V0 subunit a1 is required for a late step in synaptic vesicle exocytosis in *Drosophila*. Cell 121, 607–620.

Huang C, Chang A (2011). pH-dependent cargo sorting from the Golgi. J Biol Chem 286, 10058–10065.

Huang Y, Xie J, Wang T (2015). A fluorescence-based genetic screen to study retinal degeneration in *Drosophila*. PLoS One 10, e0144925.

Hucthagowder V, Morava E, Kornak U, Lefeber DJ, Fischer B, Dimopoulou A, Aldinger A, Choi J, Davis EC, Abuelo DN, *et al.* (2009). Loss-of-function mutations in ATP6V0A2 impair vesicular trafficking, tropoelastin secretion and cell survival. Hum Mol Genet 18, 2149–2165.

Koivusalo M, Welch C, Hayashi H, Scott CC, Kim M, Alexander T, Touret N, Hahn KM, Grinstein S (2010). Amiloride inhibits macropinocytosis by lowering submembranous pH and preventing Rac1 and Cdc42 signaling. J Cell Biol 188, 547–563.

Kornak U, Reynders E, Dimopoulou A, van Reeuwijk J, Fischer B, Rajab A, Budde B, Nurnberg P, Foulquier F, Lefeber D, *et al.* (2008). Impaired glycosylation and cutis laxa caused by mutations in the vesicular H^+-ATPase subunit ATP6V0A2. Nat Genet 40, 32–34.

Leonard R, Rendic D, Rabouille C, Wilson IB, Preat T, Altmann F (2006). The *Drosophila* fused lobes gene encodes an N-acetylglucosaminidase involved in N-glycan processing. J Biol Chem 281, 4867–4875.

Li HS, Montell C (2000). TRP and the PDZ protein, INAD, form the core complex required for retention of the signalplex in *Drosophila* photoreceptor cells. J Cell Biol 150, 1411–1422.

Liegeois S, Benedetto A, Garnier JM, Schwab Y, Labouesse M (2006). The V0-ATPase mediates apical secretion of exosomes containing Hedgehog-related proteins in *Caenorhabditis elegans*. J Cell Biol 173, 949–961.

Maxson ME, Grinstein S (2014). The vacuolar-type H(+)-ATPase at a glance—more than a proton pump. J Cell Sci 127, 4987–4993.

Nilsson T, Au CE, Bergeron JJM. (2009). Sorting out glycosylation enzymes in the Golgi apparatus. FEBS Lett 583, 3764–3769.

O'Tousa JE (1992). Requirement of N-linked glycosylation site in *Drosophila* rhodopsin. Vis Neurosci 8, 385–390.

Peters C, Bayer MJ, Buhler S, Andersen JS, Mann M, Mayer A (2001). *Trans*-complex formation by proteolipid channels in the terminal phase of membrane fusion. Nature 409, 581–588.

Poea-Guyon S, Ammar MR, Erard M, Amar M, Moreau AW, Fossier P, Gleize V, Vitale N, Morel N (2013). The V-ATPase membrane domain is a sensor of granular pH that controls the exocytotic machinery. J Cell Biol 203, 283–298.

Rosenbaum EE, Brehm KS, Vasiljevic E, Liu C-H, Hardie RC, Colley NJ (2011). XPORT dependent transport of TRP and rhodopsin. Neuron 72, 602–615.

Rosenbaum EE, Hardie RC, Colley NJ (2006). Calnexin is essential for rhodopsin maturation, Ca^{2+} regulation, and photoreceptor cell survival. Neuron 49, 229–241.

Rosenbaum EE, Vasiljevic E, Brehm KS, Colley NJ (2014). Mutations in four glycosyl hydrolases reveal a highly coordinated pathway for rhodopsin biosynthesis and N-glycan trimming in *Drosophilamelanogaster*. PLoS Genet 10, e1004349.

Satoh A, Tokunaga F, Kawamura S, Ozaki K (1997). In situ inhibition of vesicle transport and protein processing in the dominant negative Rab1 mutant of *Drosophila*. J Cell Sci 110, 2943–2953.

Satoh AK, O'Tousa JE, Ozaki K, Ready DF (2005). Rab11 mediates post-Golgi trafficking of rhodopsin to the photosensitive apical membrane of *Drosophila* photoreceptors. Development 132, 1487–1497.

Satoh T, Ohba A, Liu Z, Inagaki T, Satoh AK (2015). dPob/EMC is essential for biosynthesis of rhodopsin and other multi-pass membrane proteins in *Drosophila* photoreceptors. eLife 4, e06306.

Schopf K, Huber A (2017). Membrane protein trafficking in *Drosophila* photoreceptor cells. Eur J Cell Biol 96, 391–401.

Sobota JA, Back N, Eipper BA, Mains RE (2009). Inhibitors of the V0 subunit of the vacuolar H+-ATPase prevent segregation of lysosomal- and secretory-pathway proteins. J Cell Sci 122, 3542–3553.

Sreelatha A, Bennett TL, Carpinone EM, O'Brien KM, Jordan KD, Burdette DL, Orth K, Starai VJ (2015). Vibrio effector protein VopQ inhibits fusion of V-ATPase–containing membranes. Proc Natl Acad Sci USA 112, 100–105.

Strasser B, Iwaszkiewicz J, Michielin O, Mayer A (2011). The V-ATPase proteolipid cylinder promotes the lipid-mixing stage of SNARE-dependent fusion of yeast vacuoles. EMBO J 30, 4126–4141.

Stroupe C, Hickey CM, Mima J, Burfeind AS, Wickner W (2009). Minimal membrane docking requirements revealed by reconstitution of Rab GTPase-dependent membrane fusion from purified components. Proc Natl Acad Sci USA 106, 17626–17633.
Tsunoda S, Sierralta J, Sun Y, Bodner R, Suzuki E, Becker A, Socolich M, Zuker CS (1997). A multivalent PDZ-domain protein assembles signalling complexes in a G-protein-coupled cascade. Nature 388, 243–249.
Ungermann C, Wickner W, Xu Z (1999). Vacuole acidification is required for *trans*-SNARE pairing, LMA1 release, and homotypic fusion. Proc Natl Acad Sci USA 96, 11194–11199.
Vaccari T, Duchi S, Cortese K, Tacchetti C, Bilder D (2010). The vacuolar ATPase is required for physiological as well as pathological activation of the Notch receptor. Development 137, 1825–1832.
Van Damme T, Gardeitchik T, Mohamed M, Guerrero-Castillo S, Freisinger P, Guillemyn B, Kariminejad A, Dalloyaux D, van Kraaij S, Lefeber DJ, *et al.* (2017). Mutations in ATP6V1E1 or ATP6V1A cause autosomal-recessive cutis laxa. Am J Hum Genet 100, 216–227.
Wang D, Epstein D, Khalaf O, Srinivasan S, Williamson WR, Fayyazuddin A, Quiocho FA, Hiesinger PR (2014a). Ca^{2+}-Calmodulin regulates SNARE assembly and spontaneous neurotransmitter release via v-ATPase subunit V0a1. J Cell Biol 205, 21–31.
Wang S, Tan KL, Agosto MA, Xiong B, Yamamoto S, Sandoval H, Jaiswal M, Bayat V, Zhang K, Charng WL, *et al.* (2014b). The retromer complex is required for rhodopsin recycling and its loss leads to photoreceptor degeneration. PLoS Biol 12, e1001847.
Wang T, Jiao Y, Montell C (2005). Dissecting independent channel and scaffolding roles of the *Drosophila* transient receptor potential channel. J Cell Biol 171, 685–694.
Wang T, Jiao Y, Montell C (2007). Dissection of the pathway required for generation of vitamin A and for *Drosophila* phototransduction. J Cell Biol 177, 305–316.
Wang T, Montell C (2007). Phototransduction and retinal degeneration in *Drosophila*. Pflugers Arch 454, 821–847.
Wang T, Wang X, Xie Q, Montell C (2008). The SOCS box protein STOPS is required for phototransduction through its effects on phospholipase C. Neuron 57, 56–68.
Webel R, Menon I, O'Tousa JE, Colley NJ (2000). Role of asparagine-linked oligosaccharides in rhodopsin maturation and association with its molecular chaperone, NinaA. J Biol Chem 275, 24752–24759.
Williamson WR, Wang D, Haberman AS, Hiesinger PR (2010). A dual function of V0-ATPase a1 provides an endolysosomal degradation mechanism in *Drosophilamelanogaster* photoreceptors. J Cell Biol 189, 885–899.
Xiong B, Bayat V, Jaiswal M, Zhang K, Sandoval H, Charng WL, Li T, David G, Duraine L, Lin YQ, *et al.* (2012). Crag is a GEF for Rab11 required for rhodopsin trafficking and maintenance of adult photoreceptor cells. PLoS Biol 10, e1001438.
Xiong B, Bellen HJ (2013). Rhodopsin homeostasis and retinal degeneration: lessons from the fly. Trends Neurosci 36, 652–660.
Xu H, Lee S-J, Suzuki E, Dugan KD, Stoddard A, Li H-S, Chodosh LA, Montell C (2004). A lysosomal tetraspanin associated with retinal degeneration identified via a genome-wide screen. EMBO J 23, 811–822.
Xu Y, Wang T (2016). CULD is required for rhodopsin and TRPL channel endocytic trafficking and survival of photoreceptor cells. J Cell Sci 129, 394–405.
Yan Y, Denef N, Schupbach T (2009). The vacuolar proton pump, V-ATPase, is required for notch signaling and endosomal trafficking in *Drosophila*. Dev Cell 17, 387–402.